

QUANTITATIVE TRANSCRIPTOMIC PROFILING OF BRANCHING IN A GLYCOSPHINGOLIPID BIOSYNTHETIC PATHWAY

FROM

Hiromu Takematsu¹, Harumi Yamamoto^{1, 4}, Yuko Naito-Matsui¹, Reiko Fujinawa⁴, Kouji Tanaka^{5, 6}, Yasushi Okuno², Yoshimasa Tanaka³, Mamoru Kyogashima^{5, 6}, Reiji Kannagi⁵, Yasunori Kozutsumi^{1, 4}

Supplemental materials

Supplemental figure legends

Supplemental tables

Supplemental Figure Legends

Supplemental Figure S1

Comparison of CTxB staining among sorted GFP-positive Namalwa cells.

A. Histograms for side-by-side CTxB staining were overlaid for comparison to evaluate the inhibitory effect of wild-type or mutant *CD77Syn* expression. MFI values for CTxB staining are indicated in the right column for each sample.

B. Overlaid density plots between *CD77Syn* and *CD77Syn-TXT* cells. The GFP signal varies between and within the samples because they were of polyclonal origin of MSCV infection, whereby the strength of the GFP signal mirrors that of glycosyltransferase gene expression due to the bicistronic expression utilizing IRES. Although the MFI values of CTxB staining were more suppressed in *CD77Syn* (green) cells than in *CD77Syn-TXT* mutants (orange) on average, a similar GFP-signal, dose-dependent reduction of the CTxB signal was noted in the 2D plot, in which GFP-strong positive *CD77Syn* cells tended to show less CTxB staining. This result indicated that the difference found in the CTxB MFI values could be caused by differences in the strengths of gene expression rather than the catalytic consumption ability between these two *CD77Syn*s.

Supplemental Figure S2

Effect of CD77Syn expression in COS-7 cells.

Effect of CD77Syn expression in the ganglioside-expressed cell type different from B cells was also examined. COS-7 cells meet these criteria thus transiently co-transfected with pEF1 α (Vector), pDEST51-A4GALT (CD77Syn) or pDEST51-A4GALT-TXT (CD77Syn-TXT) in combination with pEGFP-N2. Cells were harvested with trypsinization 48 hrs after transfection and stained with anti-CD77 or CTxB-biotin as in Fig. 2. Flow cytometry was carried out and GFP-positive populations were assessed for GSL expression. Since CTxB staining was very strong in COS-7 cells, we mixed streptavidin in the ratio of PE-conjugate: non-conjugate=1:4 in this experiment to reduce the signal strength without losing linearity of the detection. Control staining from vector sample was also shown.

Supplemental Figure S3

Requirement of co-expression for co-immunoprecipitation of CD77Syn with LacCerSyn.

COS-7 cells were transiently co-transfected with *LacCerSyn-FLAG* and either control vector (NC) or *CD77Syn-HA* (PC) for immunoprecipitation with M2. When *LacCerSyn-FLAG* and *CD77Syn-HA* were separately transfected and the membrane fractions were mixed prior to immunoprecipitation (Sep), co-immunoprecipitation of these two enzymes was not detected. Immunoblotting was carried out for immunoprecipitated LacCerSyn (IP) or co-precipitated CD77Syn (Co-IP).

Anti-giantin was used as a negative control for the Golgi protein.

Supplemental Figure S4

Schematic flow model of GSL biosynthetic branching deduced from this study.

Proteins involved in GSL biosynthesis are boxed and GSL species are circled. The CD77Syn dominated in this flow model due to its “activity” to regulate the proximal enzyme, LacCerSyn, in B cells, in which CD77 expression is induced upon activation. In the absence of CD77Syn, GM3Syn dominates the branching due to channeling with LacCerSyn for ganglio-series commitment.

Supplemental Table S1

Pearson's correlation coefficient analysis of GSL staining and glycan-related gene expression profile

Pearson's correlation coefficient values (indices) of relative gene expression in the microarray versus the relative anti-CD77 staining for (A) MFI and (B) CTxB among six B cell lines calculated for glycan-related genes. A positive value indicates a positive correlation between gene expression and staining. A negative value indicates a negative correlation. *P*-values for A4GALT correlation with anti-CD77 or CTxB staining were 0.099 and 0.043, respectively. Genes expected to have roles in GSL biosynthesis are in bold.

A

Index	Gene Name	Enzyme Activity
0.971	<i>FUT6</i>	alpha (1,3) FucT-6
0.963	<i>B4GALT6</i>	LacCer synthase
0.845	<i>HS2ST1</i>	HS 2-O-SulfoT 1
0.796	<i>PIGL</i>	GPI biosynthesis, GlcNAc-PI deacetylase
0.780	<i>SLC35A1</i>	CMP-sialic acid transporter
0.774	<i>ST6GALNAC2</i>	ST6GalNAcII
0.756	<i>NDST3</i>	N-deacetylase/N-SulfoT (heparan glucosaminyl) 3
0.729	<i>A4GALT</i>	alpha (1,4) GalT/Gb3/CD77 synthase
-0.764	<i>GALNT3</i>	ppGalNAcT-3
-0.827	<i>B4GALT2</i>	beta4GalT-2
-0.854	<i>PIGM</i>	GPI biosynthesis, Man-T
-0.887	<i>PIGC</i>	GPI biosynthesis, GlcNAc-T
-0.921	<i>PAPSS2</i>	PAPS synthetase 2

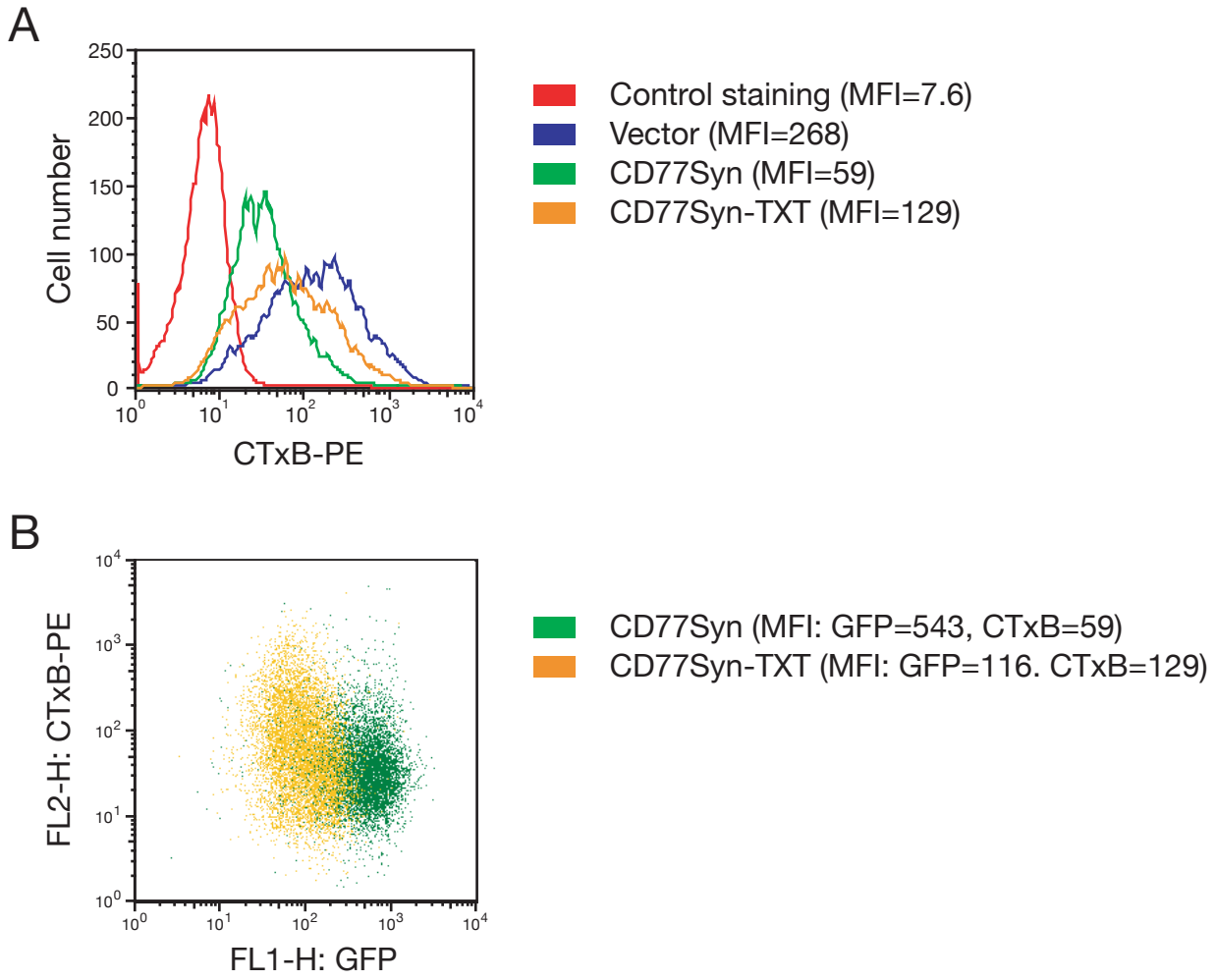
B

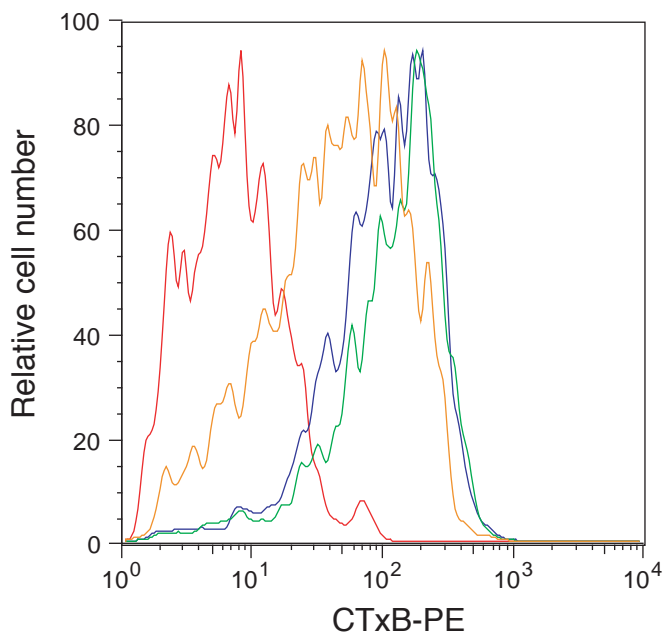
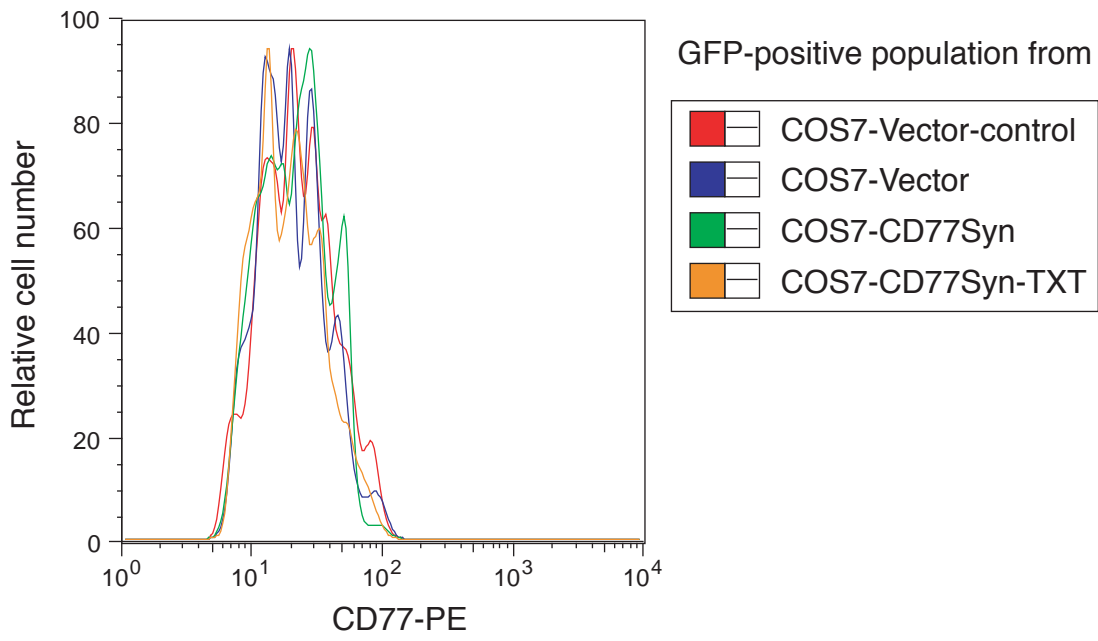
Index	Gene name	Enzyme activity
0.921	<i>UST</i>	Uronyl 2-O-sulfoT
0.836	<i>DAD1</i>	OST component
0.801	<i>EXTL1</i>	GlcNAcT for HS chain initiation and elongation
0.801	<i>NDST4</i>	N-deacetylase/N-SulfoT (heparan glucosaminyl) 4
-0.728	<i>EXTL3</i>	GlcNAcT for HS chain initiation and elongation
-0.752	<i>B3GAT1</i>	GlcAT-P
-0.753	<i>ST8SIA2</i>	ST8Sia II / STX
-0.779	<i>UGCG</i>	GlcCer synthase
-0.827	<i>A4GALT</i>	alpha (1,4) GalT/Gb3/CD77 synthase
-0.827	<i>ST3GAL4</i>	ST3Gal IV
-0.833	<i>GNE</i>	UDP-GlcNAc-2-epimerase/ManNAc kinase
-0.886	<i>PIG-B</i>	GPI biosynthesis, Dol-P-Man-dependent ManT
-0.891	<i>HS3ST2</i>	heparan sulfate 3-O-SulfoT 2
-0.939	<i>MGAT2</i>	GnT-II
-0.953	<i>ST8SIA5</i>	ST8Sia V/GD1c synthase

Supplemental Table S2.**Plasmids used in this study**

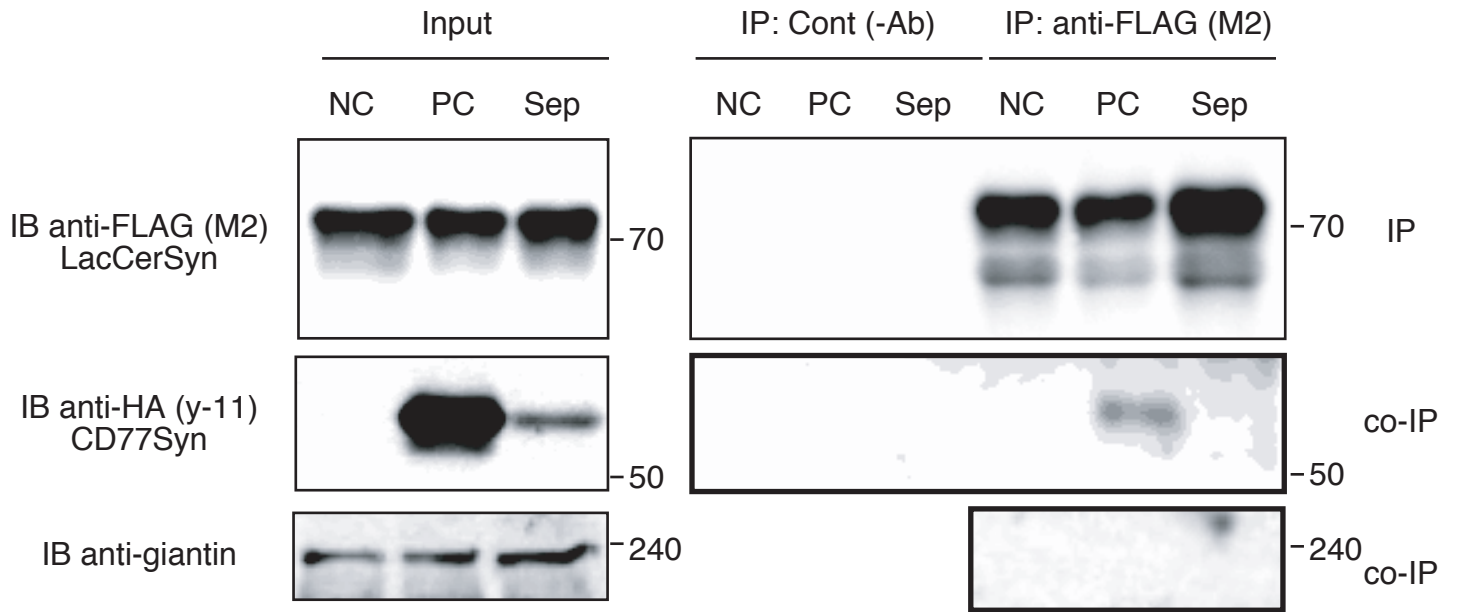
Plasmid name	cDNA	Description
pMSCV-IRES-EGFP	Control	Retrovirus vector with bicistronic expression of EGFP
pMSCV-IRES-EGFP-A4GALT	<i>A4GALT</i>	Retrovirus vector with EGFP and CD77Syn
pMSCV-IRES-EGFP-UCGT	<i>UCGT</i>	Retrovirus vector with EGFP and GlcCerSyn
pMSCV-IRES-EGFP-B4GALT6	<i>B4GALT6</i>	Retrovirus vector with EGFP and LacCerSyn
pMSCV-IRES-EGFP-ST3GAL5	<i>ST3GAL5</i>	Retrovirus vector with EGFP and GM3Syn
pMSCV-IRES-EGFP-B4GALNT4	<i>B4GALNT4</i>	Retrovirus vector with EGFP and GM2Syn
pMSCV-IRES-EGFP-B3GAL4	<i>B3GALT4</i>	Retrovirus vector with EGFP and GM1Syn
pMSCV-IRES-EGFP-B3GNT5	<i>B3GNT5</i>	Retrovirus vector with EGFP and Lc3Syn
pMSCV-IRES-EGFP-A4GALT-TXT	<i>A4GALT</i>	Retrovirus vector with EGFP and mutant CD77Syn
p3XFLAG-CMV-14	Control	Expression vector for C-terminal 3xFLAG tag with CMV promoter and neomycin resistance
p3XFLAG-CMV-14-B4GALT6	<i>B4GALT6</i>	C-terminal 3xFLAG tagged LacCerSyn
pcDNA3.1(+)	Control	Expression control vector for C-terminal 3xHA tag with CMV promoter
pcDNA3HAC-A4GALT	<i>A4GALT</i>	C-terminal 3xHA-tagged CD77Syn
pcDNA3HAC-B4GALT6	<i>B4GALT6</i>	C-terminal 3xHA-tagged LacCerSyn
pcDNA3HAC-B3GNT5	<i>B3GNT5</i>	C-terminal 3xHA-tagged Lc3Syn
pcDNA3HAC-ST3GAL5	<i>ST3GAL5</i>	C-terminal 3xHA-tagged GM3Syn
pcDNA3HAC-A4GALT-TXT	<i>A4GALT</i>	C-terminal 3xHA-tagged mutant CD77Syn
pEF1 α -V5HisA	Control	Expression vector with EF1 α promoter
pDEST51-A4GALT	<i>A4GALT</i>	CD77Syn driven from EF1 α promoter
pDEST51-A4GALT-TXT	<i>A4GALT</i>	Mutant CD77Syn driven from EF1 α promoter
pdBSP-EF-ST3GAL5-3HA-IRES-Blast	<i>ST3GAL5</i>	HA-tagged GM3Syn selectable with blasticidin
pSP72-EF-IRES-Zeo	Control	Expression vector with zeocin resistance for stable selection
pSP72-EF-A4GALT-IRES-Zeo	<i>A4GALT</i>	CD77Syn selectable with zeocin
pSP72-EF-A4GALT-TXT-IRES-Zeo	<i>A4GALT</i>	Mutant CD77Syn selectable with zeocin

Supplemental Figure S1





Supplemental Figure S3



Supplemental Figure S4

